JOURNAL OF GEOPHYSICAL RESEARCH, VOL. 98, NO. A4, PAGES 5631–5637, APRIL 1, 1993

Fine Structure of Langmuir Waves Produced by a Solar Electron Event

D. A. GURNETT, G. B. HOSPODARSKY, AND W. S. KURTH

Department of Physics and Astronomy, University of Iowa, Iowa City

D. J. WILLIAMS

Applied Physics Laboratory, Johns Hopkins University, Laurel, Maryland

S. J. BOLTON

Jet Propulsion Laboratory, Pasadena, California

Highly structured bursts of Langmuir waves produced by energetic electrons ejected from a solar flare have been observed using wideband plasma wave measurements on the Galileo spacecraft. The wideband sampling system on Galileo provides digital electric field waveforms at sampling rates up to 201,600 samples s^{-1}, much higher than any previous instrument of this type. The solar flare of interest occurred on December 10, 1990, while the spacecraft was at a radial distance of 0.98 AU from the Sun. This flare emitted a stream of energetic electrons and an associated type III radio event, both of which were detected by Galileo. Starting about 1 hour after the onset of the flare, a large number of intense Langmuir wave bursts were detected near the local electron plasma frequency, which was about 25 kHz. The Langmuir wave bursts, which lasted about 1.5 hours, coincided with the arrival of the solar electrons. The bursts are highly structured and consist mainly of isolated wave packets with durations as short as 1 ms and beat-type waveforms with beat frequencies ranging from 200 to 500 Hz. The peak electric field strengths are about 1.7 mV m^{-1}. The highly structured envelopes of these waves are strongly suggestive of nonlinear parametric decay processes such as those predicted by various theories dealing with the saturation of beam-driven electrostatic instabilities. However, the intensities are too low for strong turbulence effects to be important.

1. INTRODUCTION

For many years it has been known that type III solar radio bursts are produced by energetic electrons ejected by solar flares [*Wild*, 1950; *Lin*, 1970; *Alvarez et al.*, 1972; *Fainberg and Stone*, 1974; *Gurnett and Frank*, 1975; *Lin et al.*, 1981]. As currently understood, these radio bursts are generated by a two-step process in which electrostatic oscillations are (1) first produced by the ejected solar flare electrons via a beam-plasma instability and (2) then converted to electromagnetic radiation by nonlinear processes. The electrostatic oscillations, usually called Langmuir waves [*Tonks and Langmuir*, 1929], are excited at frequencies near the local electron plasma frequency f_p, and the radio emissions are produced at both the fundamental f_p and harmonic $2f_p$. The characteristic spectrum of a type III radio burst, consisting of an emission frequency that decreases with increasing time, is caused by the decreasing electron plasma frequency encountered by the solar flare electrons as they stream outward away from the Sun. The two-step mode conversion process was first proposed by *Ginzburg and Zheleznyakov* [1958] and was later confirmed by *Gurnett and Anderson* [1976, 1977] using measurements from the Helios spacecraft.

An important question that still remains concerning the generation of type III radio bursts is how the solar flare electrons can propagate such great distances (> 1 AU) without being disrupted by the Langmuir waves, which are in resonance with the beam. It is now widely believed that nonlinear mechanisms must act to limit the growth of the waves, thereby allowing the beam to propagate with little or no disruption. Nonlinear mechanisms that have been proposed include quasi-linear diffusion [*Magelssen and Smith*, 1977], parametric and modulational decay instabilities [*Papadopoulos et al.*, 1974; *Fried et al.*, 1976; *Bardwell and Goldman*, 1976; *Goldstein et al.*, 1979, *Smith et al.*, 1979; *Freund and Papadopoulos*, 1980], and the strongly nonlinear phenomenon of soliton collapse [*Zakharov*, 1972; *Galeev et al.*, 1975; *Wong and Quon*, 1975; *Nicholson et al.*, 1978; *Goldman et al.*, 1980; *Shapiro and Shevchenko*, 1984]. In all cases the electrostatic waves are shifted out of resonance with the beam, thereby preventing the growth of electric fields that are sufficiently intense to disrupt the beam.

Various experimental studies have been carried out to characterize the Langmuir waves responsible for the generation of the type III radio bursts [*Gurnett and Anderson*, 1976, 1977; *Gurnett et al.*, 1978, 1980; *Tokar and Gurnett*, 1980; *Lin et al.*, 1981; *Robinson et al.*, 1992*a*, *b*]. All of these studies show that the Langmuir waves involved in the generation of type III radio bursts are extremely spiky, with large-amplitude variations on time scales extending down to a small fraction of a second. These spiky intensity variations are suggestive of strongly nonlinear processes such as soliton collapse. In fact, *Kellogg et al.* [1992*a*] recently presented evidence of collapsing Langmuir wave packets at millisecond time scales using a fast envelope sampler on the Ulysses spacecraft. However, none of the available measurements have had sufficient time resolution to resolve the detailed frequency spectrum and waveform of the spiky structure. In this paper we present the first such observations.

Paper number 92JA02838.
0148-0227/93/92JA-02838$05.00

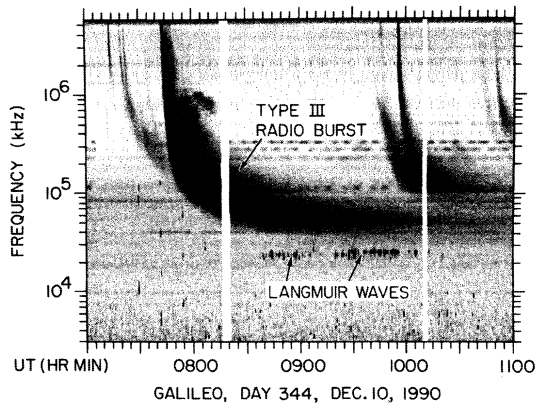

Fig. 1. This frequency-time spectrogram shows a series of type III solar radio bursts on December 10, 1990. The event of interest is the strong burst starting at 0745 UT. The bursty narrow-band emissions from 0840 to 1010 UT at about 23 kHz are the Langmuir waves responsible for generating the type III radio emissions.

The observations described are from the plasma wave and energetic particle experiments on the Galileo spacecraft, which was launched on October 18, 1989, on a somewhat circuitous trip to Jupiter that includes one gravity-assisted flyby of Venus and two gravity-assisted flybys of Earth [*Johnson et al.*, 1992]. The Galileo plasma wave experiment has several new capabilities, the most important of which is a high-rate sampling system that provides digital measurements of wideband electric field waveforms at sampling rates of 201,600 samples s^{-1}. At this sample rate, bandwidths of up to 80 kHz can be obtained with negligible aliasing. (The Nyquist frequency for a sample rate of 201,600 samples s^{-1} is 100.8 kHz.) With this system, Langmuir waves can be resolved on the smallest time scale of physical interest, which is of the order of the electron plasma period f_p^{-1}. *Gurnett et al.* [1992] provide a description of the plasma wave instrument, and *Williams et al.* [1992] describe the energetic particle instrument.

2. Description of the Event

The event of interest occurred on December 10, 1990, shortly after the first gravity-assisted flyby of Earth. The first indication of the event was from a type III solar radio burst detected by the Galileo plasma wave instrument at 0745 UT. At this time, Galileo was located on the sunward side of the Earth at a geocentric radial distance of 189.5 R_E and a local time of 9.6 hours. The heliocentric radial distance was 0.98 AU. A frequency-time spectrogram illustrating the type III radio burst is shown in Figure 1. This spectrogram is from the low-rate on-board spectrum analyzer, which provides one complete sweep of the electric field spectrum from 50 Hz to 5.6 MHz every 37.33 s. The event at 0745 UT clearly has the characteristic signature of a type III radio burst, consisting of an intense band of noise sweeping downward in frequency with increasing time. Several other somewhat weaker type III bursts can also be seen during this same period.

Comparisons with the solar flare reports listed by the *National Geophysical Data Center* [1991] show that the strong type III radio burst at 0745 UT is almost certainly associated with a type 2*F* solar flare that occurred at 15°N latitude, 47°W longitude with an onset time of 0730 UT. The location of the flare, near the equator on the west side of the Sun, placed the spacecraft in a favorable position for detecting the solar flare electrons as they streamed outward along the solar wind magnetic field lines. In fact, about 40 min after the onset of the solar flare, at about 0820 UT, the energetic particle detector on Galileo began detecting energetic electrons arriving from the direction of the Sun. The bottom panel of Figure 2 gives the electron counting rate in three energy channels, 29–42, 42–55, and 55–93 keV. The sharply peaked modulation in the counting rate, with a period of about 3 min, is caused by the azimuthal scanning of the detector and is indicative of a beamlike distribution of electrons streaming outward away from the Sun along the solar wind magnetic field lines. The anisotropy is particularly strong near the beginning of the event, from 0810 to about 0930 UT. Later in the event, after about 0945 UT, the anisotropy begins to diminish because of pitch angle scattering in the interplanetary medium.

In addition to the type III radio burst the plasma wave instrument also detected Langmuir wave emissions generated by the solar flare electron beam. The Langmuir waves can be seen in Figure 1 as a series of dark spots from 0835 to 1020 UT at about 23 kHz, which is the local solar wind electron plasma frequency. The Langmuir wave intensities are illustrated in greater detail in the middle panel of Figure 2, which shows the electric field intensities in the frequency range 21.6–25.1 kHz, which spans the local plasma frequency $f_p \simeq 23$ kHz. An effective length of 3.5 m was used

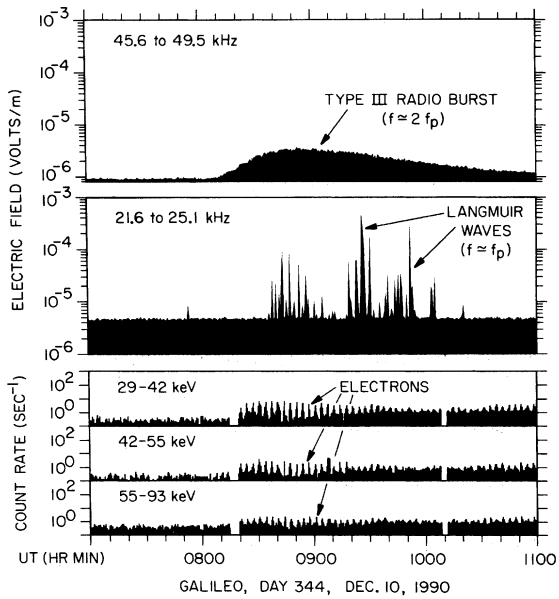

Fig. 2. (Top) Type III radio emission intensity at $f \simeq 2f_p$, (middle) Langmuir wave intensities at $f \simeq f_p$, and (bottom) the energetic solar flare electron intensities. According to the accepted theory of *Ginzberg and Zheleznyakov* [1958], the energetic electron beam excites the Langmuir waves via a beam-plasma instability, and the Langmuir waves are then converted to radio emission via nonlinear interactions.

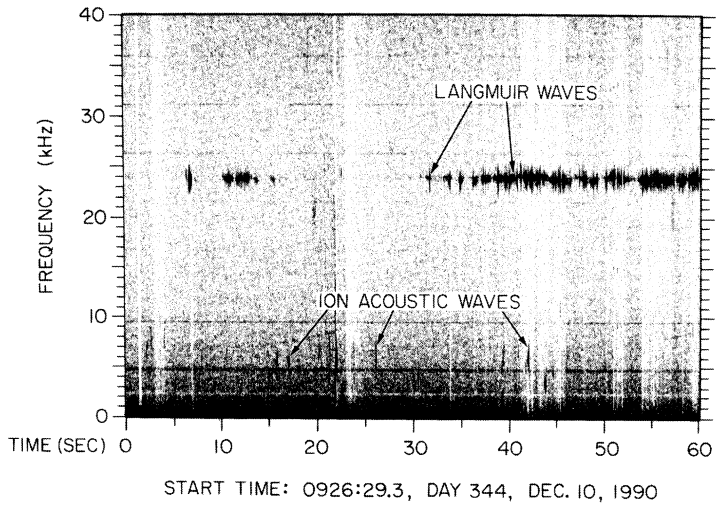

Fig. 3. A high-resolution frequency-time spectrogram during a period of relatively high Langmuir wave intensity. The Langmuir emissions have a very spiky temporal structure down to the resolution of the Fourier transform (66.67 ms) and substantial frequency spreading (up to 3 kHz). The ion acoustic waves evident in this spectrogram are not believed to be associated with the Langmuir wave emissions.

to compute the electric field strength, and no attempt was made to correct for the detailed shape of the spectrum analyzer passbands or for the antenna orientation relative to the wave vector. As can be seen, the Langmuir waves are extremely spiky. The peak electric field strengths range from a few tens of microvolts per meter to about 0.5 mV m^{-1}. These field strengths are probably underestimated, since, as will be discussed later, many of the bursts occur on short time scales compared to the integration time of the spectrum analyzer, which is about 50 ms. The onset time of the Langmuir waves at about 0835 UT corresponds roughly to the onset time of the highly anisotropic solar flare electrons, and their termination corresponds roughly to the transition from an anisotropic to a nearly isotropic distribution. This relationship is consistent with previous studies [*Lin et al.*, 1981] that show the Langmuir waves are driven by a region of positive slope, $\partial f/\partial v_{\parallel} > 0$, in the energetic electron distribution. The positive slopes are usually largest and most clearly defined early in the event. The strong Langmuir wave emissions occur in the same region where strong radio emissions are being observed at $f \simeq 2f_p$ (see the top panel of Figure 2). The good overall correspondence between the time interval at which the Langmuir waves occur and the time interval at which the $2f_p$ radio emissions occur provides strong evidence that the radio emissions are being generated at the harmonic $2f_p$, as is often the case for low-frequency type III radio bursts [*Kaiser*, 1975].

3. Langmuir Wave Structure

The fine scale structure of Langmuir wave emissions can be resolved in much greater detail using data from the wideband waveform receiver. This receiver provides four-bit samples of the electric field waveform at a variety of sampling rates. During the December 10, 1990, event the waveform sampling system was being operated in a duty cycle mode at a sampling rate of 201,600 samples s^{-1}. This mode of operation provides regularly spaced blocks of waveform data separated by constant duration gaps. For the particular combination of data transmission parameters in use at the time of this event each block of waveform data consisted of 1576 contiguous samples lasting 7.82 ms. One waveform block was being collected every 66.67 ms, with a gap of 58.85 ms between successive waveforms. The bandwidth of the antialiasing filter ahead of the analog-to-digital filter was selected to be 80 kHz. Since four-bit digitization only provides a dynamic range of 24 dB, an automatic gain control (AGC) circuit is used to control the amplitude of the signal into the analog to digital converter. The time constant of the AGC response is approximately 0.1 s, and the AGC gain is sampled once every 2.67 s.

During the roughly 2-hour interval in which Langmuir waves were being detected, approximately 91 min of high-rate electric field waveform data were received. These data are distributed more or less uniformly over the interval from 0824 to 1018 UT, thereby providing a good representative sample of the waveforms that exist through the entire event. One way to display these data is to Fourier transform each of the 7.82-ms waveform blocks and then plot the sequence of transform amplitudes in the form of a frequency-time spectrogram. An example of such a spectrogram is illustrated in Figure 3. This spectrogram shows a 1-min interval during a period of relatively high Langmuir wave activity starting at 0926:29.3 UT. The Langmuir wave emission is clearly visible at $f_p \simeq 24$ kHz. Two features are immediately apparent. First, the intensity of the Langmuir waves shows extremely rapid temporal variations, even down to the smallest time scale that can be resolved, which is the time between successive waveform blocks (66.67 ms). Second, the spectrum shows a large amount of frequency spreading, sometimes by as much as 2–3 kHz. The frequency spreading is also highly variable, sometimes changing by a factor of 5 or more between successive spectrums.

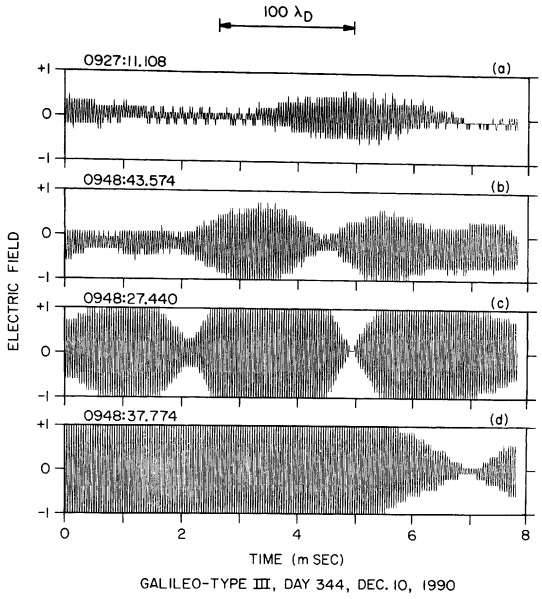

Fig. 4. Some representative Langmuir emission waveforms. Note that considerable temporal structure exists down to time scales of the order of 1 ms.

To further explore the fine scale structure, the waveforms associated with the individual 7.82-ms waveform blocks have been displayed and analyzed. Roughly 83,000 waveform blocks exist in our present data set, of which approximately 30% have clearly identifiable Langmuir wave oscillations. The waveforms show considerable variability. Figure 4 shows four waveforms that were selected to illustrate the range of phenomena observed. Each panel represents one block of waveform data. Note that the time scale is only 8 ms from the beginning to the end of each panel. The high-frequency, quasi-sinusoidal waveform evident in each of the plots is the Langmuir wave oscillation at $f = f_p$, which during these intervals is at about 24 kHz. Figure 4*a* shows an example of an isolated wave packet with a total duration of about 2 ms. Figure 4*b* shows an example of two closely spaced packets. Closely spaced wave packets of this type are fairly common. Even more striking is the occurrence of a regular string of packets, as in Figure 4*c*. Strings of packets of the type shown in Figure 4*c* are strongly suggestive of a beat between two nearly monochromatic waves of comparable amplitudes. This hypothesis has been confirmed by detailed spectrum analyses of selected waveform blocks. For example, Figure 5 shows the spectrum of the waveform in Figure 4*c*. As can be seen, the spectrum consists of two sharply defined peaks separated by about 400 Hz. The beat frequency varies somewhat from case to case but is generally in the range from 200 to 500 Hz. Beat frequencies below 200 Hz almost certainly occur, but because of the 58.85-ms gap between waveform blocks, it is difficult to determine the extent to which beats occur in this frequency range. Figure 4*d* shows a waveform that is severely clipped. This example is shown mainly to emphasize a limitation of the AGC system, which is that sometimes the gain cannot respond fast enough to the large signal amplitudes. Roughly 2% of the Langmuir oscillation waveforms display severe clipping effects of this type.

Careful inspection of the spectrogram in Figure 3 shows that in addition to the Langmuir wave emissions there are also numerous bursty emissions in the frequency range from about 3 to 10 kHz. These emissions typically have durations of a few seconds and are believed to be ion acoustic waves of the type previously discussed by *Gurnett and Anderson* [1977], *Gurnett and Frank* [1978], *Gurnett et al.* [1979], and *Kurth et al.* [1979]. Although ion acoustic waves are predicted to be generated by Langmuir waves via various parametric decay processes and have been observed in association with type III related Langmuir wave events [*Lin et al.*, 1986], the ion acoustic waves observed during this event do not appear to be related to the Langmuir wave emissions. For example, the ion acoustic wave burst at 26 s in Figure 3 occurs during a period when no Langmuir wave activity is present. This observation is consistent with previous Helios measurements [*Gurnett et al.*, 1979] that show ion acoustic waves can sometimes occur in the solar wind independently of solar flare induced Langmuir wave emissions. No Langmuir wave induced magnetic field emissions of the type reported by *Kellogg et al.* [1992*b*] were detected.

4. Electric Field Strengths

To evaluate the role of nonlinear processes, it is important to determine the maximum electric field amplitudes. As mentioned earlier, the low-rate spectrum analyzer measurements have an integration time constant (50 ms) that is too long to provide an accurate determination of the amplitude of the millisecond bursts. The only way to determine the amplitude of these bursts is via the high-rate waveform measurements. Since the high-rate waveform measurements involve an AGC, the AGC gain must be taken into account when computing the field strengths. Since the AGC time constant is only 0.1 s and the AGC gain is sampled once very 2.67 s, absolute field strengths can only be obtained during 0.1-s intervals around the times of the AGC samples. This corresponds to roughly 7% of the available waveforms. During the period of interest, a total of 2016 waveform

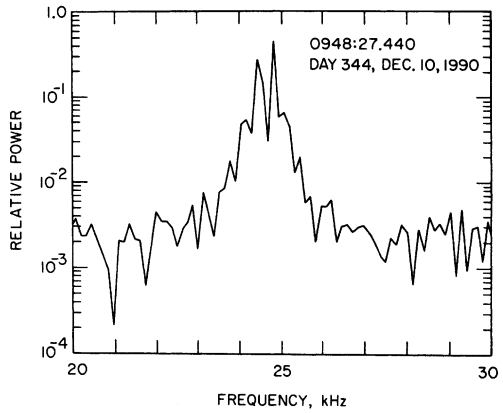

Fig. 5. A spectrum of the waveform in Figure 4*c*. The two peaks show that the modulation is caused by a beat between two waves of slightly different frequency but comparable amplitudes.

blocks have Langmuir wave emissions for which AGC gain measurements are available.

To obtain quantitative information on the distribution of field strengths, the peak electric field amplitude was determined for each 7.82-ms block of waveform data for which an AGC gain measurement was available. If the Langmuir emission waveform was not clipped, as in Figure 4*a*, then the peak amplitude was read directly from the plot. If the waveform was only moderately clipped, as in Figures 4*b* and 4*c*, then the peak amplitude was estimated by extrapolating the envelope of the waveform beyond the boundary of the plot. If the waveform was severely clipped, as in Figure 4*d*, then the peak amplitude could not be measured. For the severely clipped waveforms the clipping level was recorded. This level gives a lower limit to the electric field strength.

The distribution of peak electric field strengths obtained using the above procedure is shown in Figure 6. Two lines are shown in the plot. The solid line gives the peak field strength for waveforms that can be measured either directly (unclipped) or by extrapolation (moderately clipped), and the dashed line gives the lower limit to the field strength for the severely clipped waveforms. As can be seen, the severely clipped waveforms represent only a small fraction (~2%) of the total number of waveforms. Most of the field strengths are in the range from 0.01 to 1.0 mV m^{-1}. The sharp drop off in the number of events below 0.01 mV m^{-1} is caused by the background noise level (due to the receiver noise level and other low-level signals), which makes it difficult to measure field strengths below 0.01 mV m^{-1}. To a reasonably good approximation the amplitude distribution follows the power law $dN/(dE/E) \sim E^{-\alpha}$, where dN is the number of events in electric field interval dE. The power law index α is approximately 1 over most of the E field range, with a slight tendency to increase around 1 mV m^{-1}. The maximum field strength measured was 1.7 mV m^{-1}.

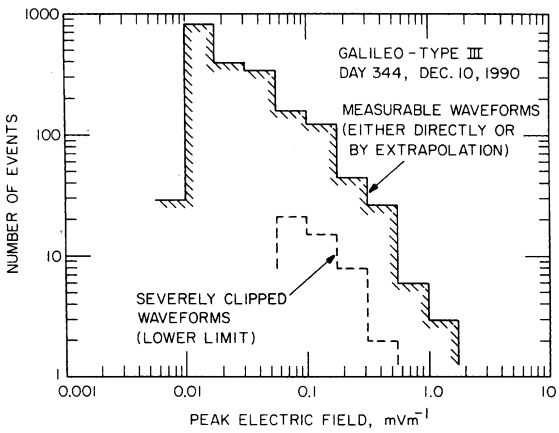

Fig. 6. The number of 7.82-ms waveform blocks as a function of the peak electric field strength. The solid line gives the distribution of peaks that can be measured either directly or by extrapolation. The dashed line gives the clipping level for severely clipped waveforms such as those in Figure 4*d*.

5. Discussion

This report describes the fine structure of Langmuir waves produced by a solar flare electron event observed by the Galileo spacecraft at a heliocentric radial distance of 0.98 AU. The structures observed span a very broad range of time scales, from tens of minutes (see Figure 2) to milliseconds (see Figure 4). If we assume that the structures are convected by the spacecraft at the nominal solar wind speed (~400 km s^{-1}), these time scales would correspond to spatial scales ranging from an upper limit of a few hundred thousand kilometers to a lower limit of a few hundred meters. At the shortest time scales involved, the waveforms consist mainly of isolated wave packets with durations of a few milliseconds and highly coherent beat-type waveforms with beat frequencies ranging from about 200 to 500 Hz. Except for the nearly constant frequency oscillation at the electron plasma frequency, little or no structure is observed on time scales of less than about 1 ms. This cutoff at about 1 ms is most likely related to the Debye length. As is well known, the smallest scale length that can occur in a plasma is controlled by the Debye length, which is given by $\lambda_D = 6.9\,(T/n)^{1/2}$ cm where T is temperature in degrees kelvin and n is the number density in cm^{-3}. Using the nominal solar wind parameters ($n = 7.1$ cm^{-3}, $V = 400$ km s^{-1}, and $T = 1.3 \times 10^5$°K), a spatial scale of 100 λ_D is shown at the top of Figure 4. As can be seen, the short scale length cutoff corresponds to a spatial scale of the order of a few tens of Debye lengths.

The isolated wave packets and beat-type waveforms are all strongly suggestive of nonlinear processes. In particular, the isolated wave packets are suggestive of the highly nonlinear phenomena of soliton collapse, and the beat-type waveforms are suggestive of parametric decay. Somewhat similar types of waveforms have been reported previously by *Gurnett et al.* [1981] upstream of Jupiter's bow shock. In evaluating the role of nonlinear processes it is usual to divide beam-plasma instabilities into two types, weak and strong, based on the ratio of the electric field energy density $E^2/8\pi$ to the plasma energy density $n\kappa T$. If $E^2/(8\pi n\kappa T) > (k\lambda_D)^2$, where k is the wave number, then the interaction is strong; otherwise, it is considered weak. In the strong interaction process a localized density decrease causes the wave energy to be focused into the density depletion. The resulting increase in the electric field pressure then leads to a further density decrease, ultimately causing the wave field to collapse into a small intense packet. Computer simulations show that the limiting size of the collapsed wave packet is of the order of a few tens of Debye lengths. Once the packet has collapsed to this size scale, the wave energy is quickly absorbed by transit-time damping, which accelerates some of the electrons to high energies. For a discussion of the collapse process, see, for example, the reviews by *Papadopoulos* [1978] or *Shapiro and Shevchenko* [1984].

The possibility that isolated wave packets of the type shown in Figure 4*a* might be the end product of a nonlinear collapse depends critically on the field strength. It is relatively straightforward to compare the observed field strength to the threshold for strongly nonlinear interactions. By using the nominal solar wind plasma parameters and $k = 2\pi/L$, where $L = 30\ \lambda_D$ is a typical scale size for the wave packet, we found the threshold electric field strength for a strong nonlinear interaction turns out to be 355 mV m^{-1}. As can be seen from Figure 6, the peak electric field strength (~1.7 mV m^{-1}) observed during this event is more than a factor of 100

below the threshold for strong nonlinear interactions. There is, of course, the possibility that some of the severely clipped waveforms could have peak field strengths well above 1.7 mV m^{-1}. However, these waveforms are exceedingly rare, and we seriously doubt that any of the waveforms could have peaks as high as 355 mV m^{-1}. Additional evidence that strong interactions are not involved is given by the frequency spectrum. As the packet collapses, the wave frequency should decrease because of the reduced plasma frequency in the density cavity. This frequency decrease should cause an asymmetric downward shift in the frequency spectrum. No such downward shift is observed. Thus it appears that strong nonlinear interactions are not responsible for generating the isolated millisecond time scale wave packets. Just what causes these wave packets is not known. The power law electric field amplitude distribution (see Figure 6) suggests that a random process may be controlling the wave amplitudes. Processes of this type have been explored by *Robinson et al.* [1992*a*, *b*], who suggested that small-scale irregularities in the solar wind cause stochastic fluctuations in the growth rate. Whether stochastic fluctuations can explain the existence of isolated wave packets down to millisecond time scales depends critically on the density structure of the solar wind at very small spatial scales (a few kilometers or less). Unfortunately, very little is known about density fluctuations in the solar wind at such short length scales.

Beat-type waveforms of the type illustrated in Figures 4*b* and 4*c* are almost certainly caused by interference between two waves of slightly different frequency but similar amplitude. Modulated waveforms of this type have been observed previously in the electron foreshock at Jupiter [*Gurnett et al.*, 1981]. Parametric decay seems to provide the most obvious explanation of these waveforms. In contrast to the collapsed wave packets, parametric decay is inherently a weak interaction process and does not involve large field strengths. Although other processes such as the excitation of waves by beams of different velocities could lead to the generation of two or more waves, only the parametric decay process provides a credible explanation for the fact that the two waves always seem to have comparable amplitudes. In the parametric decay process a beam-driven Langmuir wave, ω_1 decays into a second Langmuir wave ω_2 and a low-frequency wave ω_L. For a discussion of this process, see the work by *Fried et al.* [1976]. The three waves must satisfy the conditions of conservation of energy, $\omega_1 = \omega_2 + \omega_L$, and conservation of momentum, $\mathbf{k}_1 = \mathbf{k}_2 + \mathbf{k}_L$. Recently, *Cairns and Robinson* [1992] have developed a theory for computing the beat frequency that takes into account the Doppler shift of the two Langmuir waves due to the motion of the solar wind. The observed beat frequency (a few hundred hertz) appears to be in reasonable agreement with their predictions for beam speeds of $v_b \sim 10^8$ m/ s^{-1}, which are typical of the beam velocities involved in this event. Since the beat frequency is well below the ion plasma frequency, the low-frequency wave is almost certainly an ion acoustic wave. Although ion acoustic waves have been observed in association with type III related Langmuir wave events [*Lin et al.*, 1986], no ion acoustic waves were observed. We have no clear explanation for the absence of ion acoustic waves during this event. One possibility is simply sensitivity. The length of the Galileo electric antenna, 6.6 m tip to tip, is considerably shorter than the antenna used by *Lin et al.* [1986], which was 90 m tip to tip. Since ion acoustic waves associated with Langmuir wave emissions are relatively weak, 10^{-5}–10^{-4} V/m^{-1}, it may be that the intensities were simply too small to be detected by Galileo.

Acknowledgments. The authors would like to thank Lisa Wainio of the Jet Propulsion Laboratory for her efforts in getting the wideband data to us. We also thank Larry Granroth and Scott Allendorf for their efforts in carrying out the data processing. This research was supported by NASA contract 958779 with the Jet Propulsion Laboratory.

The Editor thanks R. J. Strangeway and R. P. Lin for their assistance in evaluating this paper.

REFERENCES

Alvarez, H., F. T. Haddock, and R. P. Lin, Evidence for electron excitation of type III radio burst emission, *Sol. Phys.*, *26*, 468, 1972.

Bardwell, S., and M. V. Goldman, Three-dimensional Langmuir wave instabilities in type III solar radio bursts, *Astrophys. J.*, *209*, 912, 1976.

Cairns, I. H., and P. A. Robinson, Theory for low-frequency modulated Langmuir wave packets, *Geophys. Res. Lett.*, *19*, 2187, 1992.

Fainberg, J., and R. G. Stone, Satellite observations of type III solar radio bursts at low frequencies, *Space Sci. Rev.*, *16*, 145, 1974.

Freund, H. P., and K. Papadopoulos, Oscillating two-stream and parametric decay instability in a weakly magnetized plasma, *Phys. Fluids*, *23*, 139, 1980.

Fried, B. D., T. Ikemura, K. Nishikawa, and G. Schmidt, Parametric instabilities with finite wavelength pump, *Phys. Fluids*, *19*, 1975, 1976.

Galeev, A. A., R. Z. Sagdeev, Yu. S. Sigov, V. D. Shapiro, and V. I. Shevchenko, Nonlinear theory for the modulational instability of plasma waves, *Sov. J. Plasma Phys.* Engl. Transl., *1*, 5, 1975.

Ginzburg, V. L., and V. V. Zheleznyakov, On the possible mechanism of sporadic solar radio emission (radiation in an isotropic plasma), *Sov. Astron.*, Engl. Transl., *AJ2*, 653, 1958.

Goldman, M. V., G. F. Reiter, and D. R. Nicholson, Radiation from a strongly turbulent plasma: Application to electron beam-excited solar emissions, *Phys. Fluids*, *23*, 388, 1980.

Goldstein, M. L., R. A. Smith, and K. Papadopoulos, Nonlinear stability of solar type III radio bursts, II, Application to observations near 1 A.U., *Astrophys. J.*, *234*, 683, 1979.

Gurnett, D. A., and R. R. Anderson, Electron plasma oscillations associated with type III radio bursts, *Science*, *194*, 1159, 1976.

Gurnett, D. A., and R. R. Anderson, Plasma wave electric fields in the solar wind: Initial results from Helios 1, *J. Geophys. Res.*, *82*, 632, 1977.

Gurnett, D. A., and L. A. Frank, Electron plasma oscillations associated with type III radio emissions and solar electrons, *Sol. Phys.*, *45*, 477, 1975.

Gurnett, D. A., and L. A. Frank, Ion acoustic waves in the solar wind, *J. Geophys. Res.*, *83*, 58, 1978.

Gurnett, D. A., R. R. Anderson, F. L. Scarf, and W. S. Kurth, The heliocentric radial variation of plasma oscillations associated with type III radio bursts, *J. Geophys. Res.*, *83*, 4147, 1978.

Gurnett, D. A., E. Marsch, W. Pilipp, R. Schwenn, and H. Rosenbauer, Ion acoustic waves and related plasma observations in the solar wind, *J. Geophys. Res.*, *84*, 2029, 1979.

Gurnett, D. A., R. R. Anderson, and R. L. Tokar, Plasma oscillations and the emissivity of type III radio bursts, in *Radio Physics of the Sun*, edited by M. R. Kundu and T. E. Gergely, p. 369, D. Reidel, Norwell, Mass., 1980.

Gurnett, D. A., J. E. Maggs, D. L. Gallagher, W. S. Kurth, and F. L. Scarf, Parametric interaction and spatial collapse of beam-driven Langmuir wave in the solar wind, *J. Geophys. Res.*, *86*, 8833, 1981.

Gurnett, D. A., W. S. Kurth, R. R. Shaw, A. Roux, R. Gendrin, C. F. Kennel, F. L. Scarf, and S. D. Shawhan, The Galileo plasma wave investigation, *Space Sci. Rev.*, *60*, 341, 1992.

Johnson, T. V., C. M. Yeates, and R. Young, Space science reviews volume on Galileo mission overview, *Space Sci. Rev.*, *60*, 3, 1992.

Kaiser, M. L., The solar elongation distribution of low frequency radio bursts, *Sol. Phys.*, *45*, 181, 1975.

Kellogg, P. J., K. Goetz, R. L. Howard, and S. J. Monson, Evidence for Langmuir wave collapse in the interplanetary plasma, *Geophys. Res. Lett.*, *19*, 1303, 1992*a*.

Kellogg, P. J., K. Goetz, N. Lin, S. J. Monson, A. Balogh, R. J. Forsyth, and R. G. Stone, Low-frequency magnetic signals associated with Langmuir wave, *Geophys. Res. Lett.*, *19*, 1299, 1992*b*.

Kurth, W. S., D. A. Gurnett, and F. L. Scarf, High-resolution spectrograms of ion acoustic waves in the solar wind, *J. Geophys. Res.*, *84*, 3413, 1979.

Lin, R. P., The emission and propagation of 40 keV solar flare electrons, *Sol. Phys.*, *12*, 266, 1970.

Lin, R. P., D. W. Potter, D. A. Gurnett, and F. L. Scarf, Energetic electrons and plasma waves associated with a solar type III radio burst, *Astrophys. J.*, *251*, 364, 1981.

Lin, R. P., W. K. Levedal, W. Lotko, D. A. Gurnett, and F. L. Scarf, Evidence for nonlinear wave-wave interactions in solar type III radio bursts, *Astrophys. J.*, *308*, 954, 1986.

Magelssen, G. R., and D. F. Smith, Non relativistic electron stream propagation in the solar atmosphere and type III radio bursts, *Sol. Phys.*, *55*, 211, 1977.

National Geophysical Data Center, Solar-geophysical data prompt reports, *Rep. 557-Part 1*, Boulder, Colo., Jan. 1991.

Nicholson, D. R., M. V. Goldman, P. Hoyng, and J. C. Weatherall, Nonlinear Langmuir waves during type III solar radio bursts, *Astrophys. J.*, *223*, 605, 1978.

Papadopoulos, K., On the physics of strong turbulence for electron plasma waves, in *Proceedings of the Varenna School on Plasma Physics*, p. 355, Pergamon, New York, 1978.

Papadopoulos, K., M. L. Goldstein, and R. A. Smith, Stabilization of electron streams in type III solar radio bursts, *Astrophys. J.*, *196*, 175, 1974.

Robinson, P. A., I. H. Cairns, and D. A. Gurnett, Correlation between density fluctuations and clumpy Langmuir wave in type III radio sources, *Astrophys. J.*, in press, 1992*a*.

Robinson, P. A., I. H. Cairns, and D. A. Gurnett, Clumpy Langmuir wave in type III radio sources: Comparison of stochastic-growth theory with observations, *Astrophys. J.*, in press, 1992*b*.

Shapiro, V. D., and V. I. Shevchenko, Strong turbulence of plasma oscillations, in *Handbook of Plasma Physics*, vol. 2, *Basic Plasma Physics*, edited by A. A. Galeev and R. N. Sudan, p. 124, North-Holland, New York, 1984.

Smith, R. A., M. L. Goldstein, and K. Papadopoulos, Nonlinear stability of solar type III radio bursts, I, Theory, *Astrophys. J.*, *234*, 348, 1979.

Tokar, R. L., and D. A. Gurnett, The volume emissivity of type III radio bursts, *J. Geophys. Res.*, *85*, 2353, 1980.

Tonks, L., and I. Langmuir, Oscillations in ionized gases, *Phys. Rev.*, *33*, 195, 1929.

Wild, J. P., Observations of the spectrum of high-intensity solar radiation at metre wavelengths, III, Isolated bursts, *Aust. J. Sci. Res., Ser. A*, *3*, 541, 1950.

Williams, D. J., R. W. McEntire, S. Jaskulek, and B. Wilken, The Galileo energetic particles detector, *Space Sci. Rev.*, *60*, 385, 1992.

Wong, A. Y., and B. H. Quon, Spatial collapse of beam-driven plasma waves, *Phys. Rev. Lett*, *34*, 1499, 1975.

Zakharov, V. E., Collapse of Langmuir waves, *Sov. Phys. JETP*, Engl. Transl. *35*, 908, 1972.

S. J. Bolton, Jet Propulsion Laboratory, 4800 Oak Grove Drive, Pasadena, CA 91109.

D. A. Gurnett, G. B. Hospodarsky, and W. S. Kurth, Department of Physics and Astronomy, University of Iowa, Iowa City, IA 52242.

D. J. Williams, Applied Physics Laboratory, Johns Hopkins University, Laurel, MD 20723.

(Received August 19, 1992;
revised November 24, 1992;
accepted November 25, 1992.)